Journal of *Marine Science and Engineering*

Article

Operational Strategy Optimization of LNG Dual-Fuel Ships Considering Emission Regulations and Carbon Tax

Qin Wang *, Sinuo Liu and Wenzhen He

College of Transport and Communications, Shanghai Maritime University, Shanghai 201306, China
* Correspondence: qinwang@shmtu.edu.cn

Abstract

The liner shipping industry is thriving in the low-carbon transition, and optimizing operational strategies for liquefied natural gas (LNG) dual-fuel ships has become a research hotspot. This research examines the impacts of the carbon tax, emission control area (ECA) policies, fuel price discounts and methane slip rate on fuel management strategies. Firstly, to reduce liner operating costs and adhere to ECA policies, this study develops a basic optimization model. Further, the model is extended to take into account the impact of fuel price discounts. Secondly, by linearizing multiple nonlinear terms, the operational strategies are obtained. Thirdly, taking a real vessel sailing between the Far East and Northwest Europe as a case study, this study identifies the ports for LNG and very low sulfur fuel oil (VLSFO) bunkering, determines the bunkering amounts and calculates the planned speeds. Furthermore, sensitivity analyses are conducted on fuel price difference, carbon tax rate and methane slip rate. Results show that fuel price difference, carbon tax rate, methane slip rate and fuel price discount exert a significant impact on ship operational decisions. To ensure the effectiveness of maritime decarbonization regulations, authorities should monitor ship engines with high methane slip rates. This study offers important references for shipping enterprises to meet ship emission policies and simultaneously cut operational costs.

Keywords: ship emission regulations; green shipping; LNG; maritime decarbonization; carbon tax

1. Introduction

As trade becomes increasingly globalized, liner transportation is playing a crucial role in global trade [1]. However, shipping activities generate atmospheric pollutants, seriously harming the environment. According to the data released by the International Maritime Organization (IMO), the reported greenhouse gas emissions in 2018 increased by 9.6% compared to 2012 [2]. To further reduce pollutant emissions from ships, relevant organizations of various countries have released a series of strict regulations [3]. In 2020, China announced the 'dual carbon' goals to combat global climate change, striving to achieve a carbon peak by 2030.

To reduce sulfur oxides, the IMO enforces the ECA policy in the Mediterranean Sea. The sulfur content limits for ship fuel within and outside the ECA are 0.1% m/m and 0.5% m/m, respectively, as shown in Table 1. To comply with sulfur limit regulations, shipping companies mainly use LNG alternative fuel, install exhaust gas scrubbers, and conduct fuel switching [4,5]. The extremely low sulfur content of LNG enables nearly zero sulfur oxide emissions, making it fully compliant with ECA regulations. However, the sulfur

Check for updates

Academic Editor: Juan Moreno-Gutiérrez

Received: 26 February 2026
Revised: 19 March 2026
Accepted: 21 March 2026
Published: 26 March 2026

content of VLSFO cannot exceed 0.50% m/m, and it can be used outside 0.1% sulfur ECAs. Fuel switching technology refers to ships switching between conventional and low-sulfur fuel when entering or exiting the ECAs. This method is popular among many shipping companies due to the low complexity. Kouzelis et al. [6] developed a decision support tool for selecting alternative fuel technologies and reducing shipping costs. Li et al. [7] took methanol dual-fuel powered ships as a case study and developed a model that jointly optimizes route and speed to reduce operational costs and emissions. The results show that increasing methanol fuel tank capacity can improve economic benefits. Wu et al. [8] considered factors such as fuel price fluctuations, carbon tax, fuel consumption and port fuel supply, and proposed a multi-stage stochastic programming model. The results show that fuel prices affect bunkering decisions for low-sulfur fuel.

Table 1. The sulfur limit in the Mediterranean ECA [9].

Category	Limit	Applicability
Sulfur oxides	0.50% sulfur (m/m)	Outside the ECA
Sulfur oxides	0.10% sulfur (m/m)	Within the ECA

1.1. Literature Review

Shipping companies can reduce emissions through technologies, operational strategies and market means [10–12]. Using alternative fuels is recognized as a promising approach [13], and several alternative fuels exhibit great potential in terms of environmental advantages. A life cycle assessment approach is adopted to identify the most promising alternative fuels [14]. Tu et al. [15] evaluated the economic viability and emission reduction potential of commonly used alternative fuels. Marine diesel engines are an important source of ship exhaust, and the cost of retrofitting traditional ships with alternative fuels is relatively low [16]. Marine clean fuels currently used include methanol, LNG, biofuels, ammonia and hydrogen. Milojević et al. [17] conducted a study dedicated to the design, maintenance and safety challenges of biomethane vehicles. Based on a comprehensive assessment of economics, technology maturity, availability and emission reduction effects, LNG shows significant advantages. As a technically mature transition fuel, LNG can effectively help the shipping enterprises comply with current emission regulations [18]. The global LNG supply shows steady growth, with export volumes of 356 million tons in 2020, increasing to 399.6 million tons in 2022, and recently reaching approximately 406 million tons in 2023 [19,20]. The growth in global natural gas demand has brought a significant increase in LNG maritime trade volumes, leading to the expansion of the LNG carrier fleet and an increase in new ship orders, while LNG-powered ships are also experiencing rapid development in the liner shipping service.

In recent years, research on operational strategies of LNG-dual-fuel ships has increased substantially. He et al. [21] included fuel price uncertainty in their research, constructing an optimization model for fuel switching and speeds. Results demonstrate that fuel switching can help cut the total operational costs of LNG dual-fuel ships. A nonlinear optimization model was developed by Gu et al. [22] by taking into account sulfur emission regulations and fuel price uncertainty. They concluded that investing in LNG-fueled ships can effectively reduce pollutant emissions. Focusing on LNG tramp vessels, He et al. [23] formulated a strategic optimization model. Research findings indicate that refueling at an alternative port can effectively reduce overall operational costs when substantial price differences exist among ports. Integrating ECA policies and the 'European Union Emissions Trading System' (EU ETS), Shih et al. [24] constructed an optimization model for LNG dual-fuel ship operations. Then, a genetic algorithm was proposed to solve the problem, with the objective of lowering the total cost and carbon dioxide (CO_2) emissions. Finally, the fuel ratio and planned speeds for ships are obtained.

LNG is a clean fuel commonly used in maritime transportation, leading to a continuously increasing number of LNG-powered vessels operating globally. However, methane slip can also occur when using LNG [25]. Methane slip represents the unburned methane escaping from LNG ship engines. In addressing the methane slip issue, scholars mainly focus on engine technology innovation, after-treatment technologies, and operational strategy optimization [26]. Lim et al. [27] combined steam methane reforming with onboard hydrogen production on LNG-powered vessels to reduce the negative environmental impact of methane. Kuittinen et al. [28] take an LNG-powered cruise ship as a case study, surprisingly finding that methane slip increases significantly at low-load conditions. Zarrinkolah and Hosseini [29] found that switching fuels and optimizing fuel injection angles can reduce methane slip from mixed-fuel engines. In terms of operational management strategies, scholars have conducted in-depth analyses of fuel types and operational speeds. However, many studies have overlooked the combined impact of fuel price discounts and methane slip on operational costs [30]. Only a few studies have focused on the methane slip issue. For example, Wu et al. [31] considered factors such as methane slip, fuel consumption, and CO_2 emissions to optimize the fuel bunkering volume of LNG. The results show that methane slip affects the selection of the fuel type and bunkering amount. Shangguan et al. [30] considered the impact of methane slip on total costs and found that incorporating methane slip considerations in LNG dual-fuel vessel management helps reduce economic losses. Hybrid propulsion systems offer certain advantages in terms of saving fuel and cutting pollutant emissions [32]. Targeting hybrid power systems, Milićević et al. [33] employed numerical analysis to investigate the effect of critical design parameters on the system efficiency. It is shown that hybrid propulsion systems substantially influence fuel consumption.

1.2. Objectives and Contributions

LNG dual-fuel ships are selected as the research subject in this study, in which methane is stored as LNG and used together with VLSFO. Compared with previous studies, the contribution of this study mainly lies in three aspects. Firstly, the previous literature did not simultaneously include the combined effects of price discounts, methane slip, carbon tax and ECA policies, fixed operating costs, and time window constraints on operational strategies. However, this research incorporates all these factors, ensuring the model's generality. Secondly, to improve the computational feasibility of the proposed models, multiple nonlinear terms have been linearized, which has theoretical implications. Thirdly, to analyze the effect of key factors on the operational decisions, sensitivity analyses were carried out on fuel price difference, carbon tax rate and methane slip rate, based on actual liner service data. Overall, this research has made significant contributions in three aspects: the generality of the model, linearization of multiple nonlinear terms and optimization of operational strategies. This research will enrich the theories of fuel bunkering strategies and planned speeds for LNG dual-fuel ships, consistent with the trend towards a green transition in global shipping, and provide assistance for liner companies to make fuel bunkering decisions. The construction of the fuel bunkering optimization models helps reduce total costs and carbon emissions in liner shipping.

The rest of the sections are shown as follows. Section 2 presents two optimization models, while Sections 3 and 4 detail the linearization approach and case analyses. Section 5 provides the primary conclusions. Figure 1 depicts the research framework.

https://doi.org/10.3390/jmse14070615

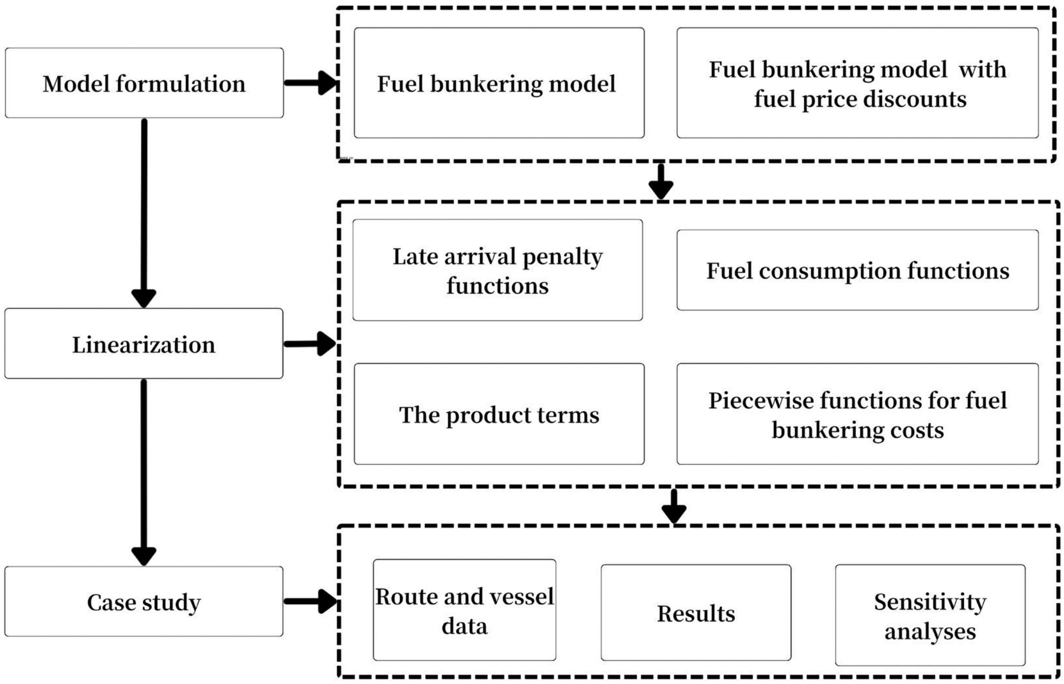

Figure 1. Research framework.

2. Model Formulation

2.1. Problem Description and Assumptions

2.1.1. Problem Description

The research analyzes an ocean-going route that involves several port stops and ECAs. The liner company has deployed some ships to maintain the normal operation of weekly liner service. It is assumed that there are n ports on this route, with the port set denoted as $P = \{1, 2, 3, \ldots, n\}$. The leg i connects port i to port $(i + 1)$, and port $(n + 1)$ is identical to the origin. In other words, the liner vessel departs from port 1 and eventually returns to the initial port, thus forming a closed-loop round voyage. During the transportation, liner ships may navigate at lower speeds within ECAs, which could result in an increased voyage time. Meanwhile, vessel operations are constrained by port arrival-time windows. This study employs soft time windows. If a liner vessel arrives late, a late arrival penalty is imposed. The delay penalties may incentivize vessels to increase operational speeds. However, excessively high speeds lead to increased carbon emissions, which in turn result in a higher carbon tax. Therefore, vessels need to strike a balance between low speeds and high service levels.

Due to the long voyage distance of ocean-going routes, container ships need to refuel at ports of call. When selecting bunkering ports, LNG dual-fuel powered vessels must consider aspects such as the availability of LNG refueling facilities, fuel types, fuel prices and even weather conditions. This study ignores emergency situations such as severe weather and assumes that all ports can supply conventional fuels such as VLSFO, while only a few ports are capable of supplying LNG. Since the ignition temperature of LNG is higher than that of traditional fuel oil, a small amount of conventional fuel is required for ignition. Thus, for LNG dual-fuel powered container ships, the consumption of pilot fuel should be considered and constrained. Given that fuel prices, bunkering facilities and bunkering capacity vary across different ports, it is necessary to select appropriate bunkering ports and bunkering amounts to formulate a reasonable bunkering strategy, with the purpose to reduce the operational costs of ships.

2.1.2. Compliance Mechanism and Modeling Framework

This study comprehensively considers the effect of ship emission regulations on shipping companies' operational decisions, including carbon tax policies and ECA regulations. Firstly, in the study, compliance with ECA regulations is considered a hard constraint. Thus, it is assumed that LNG dual-fuel powered ships burn LNG within ECAs. At ports outside of ECAs, shipping companies can choose to refuel with VLSFO (sulfur content $\leq$ 0.50%) or LNG, and the bunkering volume is mainly influenced by fuel prices. Second, the European Union has released carbon tax regulations for certain types of ships. While meeting ECA policies, shipping companies urgently need to reduce carbon taxes and total costs.

The research incorporates both methane slip and carbon emissions from the burning of LNG and VLSFO into the objective function to quantify the real costs imposed on shipping companies by ECA limitations and carbon tax policies. Meanwhile, this study provides shipping companies with optimized operational strategies, including the determination of bunkering ports, refueling volumes, fuel types and planned speeds.

2.1.3. Assumptions

The basic model is proposed on the following 4 assumptions:

Assumption 1. *The ports of call on the route and the sequence are known.*

Assumption 2. *The liner ships assigned to the route are of a similar type. Only the bunker fuel consumed by the main engines is considered.*

Assumption 3. *The departure frequency is once a week [34,35]. Liner ships only refuel at ports of call, with bunker prices being known.*

Assumption 4. *The fuel switching time at ECA boundaries is not considered [36].*

2.2. A List of the Notations

(1) Indices and sets
$P = \{1, 2, \ldots, n\}$: A set contains ports of call.
P_{LNG}: A set of ports that support LNG bunkering.
P_{NON}: A set of ports without LNG bunkering facilities.
R: A set of voyage legs.
R_E: A set of voyage legs within ECAs.
R_N: A set of voyage legs outside ECAs.
Z^*: A set of non-negative integers.
(2) Parameters
d_i^E: ECA distance on leg i of the route, nm.
d_i^N: Non-ECA distance on leg i of the route, nm.
t_i: Berthing time at the *i-th* port, h.
T_i^a: Actual arrival time at the *i-th* port, h.
T_i^E: Latest arrival time at the *i-th* port, h.
T: End time of the time window, h.
v_0: Design speed, kn.
v_{max}: Maximum speed, kn.
v_{min}: Minimum speed, kn.
p_i^L: LNG fuel price at the *i-th* port, USD/ton.
p_i^V: VLSFO fuel price at the *i-th* port, USD/ton.
C_g: Fuel bunkering cost for each operation, USD.
H_L: The upper limit of LNG tank capacity, ton.
H_V: The upper limit of VLSFO tank, ton.
s: Maximum number of bunkering operations.

α: Safety stock ratio.
β: Pilot fuel ratio.
γ: Carbon emission factor of LNG, $g\ CO_2/g\ fuel$.
θ: Carbon emission factor of VLSFO, $g\ CO_2/g\ fuel$.
ε: Late arrival penalty per hour, USD/h.
p_c: Carbon tax rate, USD/ton.
p_m: Methane slip tax rate, USD/ton.
k_{max}: Maximum number of ships deployed.
SF^M: Main engine fuel consumption rate, g/(kW·h).
EL^M: Load factor of main engine.
PS^M: Main engine nominal power, kW.
F^M: Main engine specific fuel consumption coefficient, ton/h.
φ: Heat value conversion factor from marine fuel to LNG.
$F(v_i^E)$, $F(v_i^N)$: Main engine fuel consumption function within/outside ECAs.
σ: Methane slip rate per hour, ton/h.
B_1: Bunkering amount threshold for the first fuel discount, $B_1 \geq 0$, ton.
B_2: Bunkering amount threshold for the second fuel discount, $B_2 \geq 0$, ton.
λ_1: Price discount rate when bunkering amount lies within $(B_1, B_2], \lambda_1 \geq 0$.
λ_2: Price discount rate when bunkering amount exceeds $B_2, 0 \leq \lambda_2 \leq \lambda_1 \leq 1$.
C_0: Weekly fixed operating cost of a liner ship, USD.
δ_i: Price difference between LNG and VLSFO, USD/ton.
w_0: Fuel onboard at departure.
(3) Variables
v_i^E: Speed on leg i within ECAs, kn.
v_i^N: Speed on leg i outside ECAs, kn.
Q_i^L: LNG bunkering amount at port i, ton.
Q_i^V: VLSFO bunkering amount at the *i-th* port, ton.
x_i^L: $x_i^L = 1$ if LNG bunkering is conducted at the *i-th* port, otherwise $x_i^L = 0$.
x_i^V: $x_i^V = 1$ if VLSFO bunkering is conducted at the *i-th* port, otherwise $x_i^V = 0$.
y_i: $y_i = 1$ if VLSFO is used as fuel on leg i outside ECAs, $y_i = 0$ if LNG is used.
k: Number of liner vessels assigned to the route.
(4) Functions
w_i^L: Arrival LNG stock at port i, ton.
w_i^V: Arrival VLSFO stock at port i, ton.
FP_i^V: Ignition fuel consumption on voyage leg i, ton.
F_i^L: Total LNG fuel consumption on voyage leg i, ton.
F_i^V: Total VLSFO fuel consumption on voyage leg i, ton.
C_i^L: LNG bunkering cost with fuel price discounts, USD.
C_i^V: VLSFO bunkering cost with fuel price discounts, USD.

2.3. Fuel Bunkering Model for LNG Dual-Fuel Powered Vessels

2.3.1. Fixed Operating Cost

The fixed operating cost during the navigation refers to the cost incurred to maintain normal operation that is not affected by navigation conditions. The aggregate fixed operating cost per round trip can be formulated as kC_0 [34,37].

2.3.2. Fuel Bunkering Cost

LNG dual-fuel powered vessels refuel at ports of call. Therefore, the fuel bunkering cost for a round voyage is determined by fuel prices and bunkering amounts. In addition, fixed cost per bunkering is generated during the bunkering process [38]. Dual-fuel powered liners can use LNG and VLSFO as fuels. Thus, the LNG and VLSFO fuel bunkering costs can be written as $\sum_{i=1}^{n}(p_i^L Q_i^L x_i^L + C_g x_i^L)$ and $\sum_{i=1}^{n}(p_i^V Q_i^V x_i^V + C_g x_i^V)$. Therefore, the total fuel bunkering cost for an LNG dual-fuel powered vessel on a round voyage can be expressed as $\sum_{i=1}^{n}[p_i^L Q_i^L x_i^L + p_i^V Q_i^V x_i^V + C_g(x_i^L + x_i^V)]$.

2.3.3. Carbon Tax

The fuel consumption of LNG dual-fuel ships during navigation mainly comes from the main engine, where methane slip occurs. Based on the principle of heating value conservation, the LNG volumes consumed by main engines within and outside ECAs are $\varphi F(v_i^E)$ and $\varphi F(v_i^N)$, respectively [39], where $F(v_i^E)$ and $F(v_i^N)$ represent the main engine fuel consumption within and outside ECAs, respectively, as shown below

$$F(v_i^E) = F^M(\frac{v_i^E}{v_0})^3 \frac{d_i^E}{v_i^E} \tag{1}$$

$$F(v_i^N) = F^M(\frac{v_i^N}{v_0})^3 \frac{d_i^N}{v_i^N} \tag{2}$$

$$F^M = SF^M EL^M PS^M 10^{-6} \tag{3}$$

where SF^M is equal to 206 g/(kW·h) , EL^M denotes the main engine operating load factor with a value of 0.8, and PS^M represents the main engine rated power [40,41].

LNG dual-fuel powered vessels can choose to use either LNG or VLSFO when operating outside ECAs. When $y_i = 0$, the vessel uses LNG outside ECAs; otherwise, VLSFO is used. On voyage leg i, the main engines may consume LNG and VLSFO. Specifically, the LNG consumption within and outside ECAs on leg i are $\varphi F(v_i^E)$ and $\varphi F(v_i^N)(1 - y_i)$, respectively, and the VLSFO consumption outside ECAs is $F(v_i^N)y_i$. Since LNG has a higher ignition temperature, it typically requires 1–3% pilot fuel for ignition [42,43]. Let the pilot fuel consumption be FP_i^V, and according to [44], it is obtained that

$$FP_i^V = \beta\varphi[F(v_i^E) + F(v_i^N)(1 - y_i)] \tag{4}$$

The aggregate LNG and VLSFO fuel consumption on voyage leg i are denoted as F_i^L and F_i^V, respectively. Hence

$$F_i^L = \varphi F(v_i^E) + \varphi F(v_i^N)(1 - y_i) \tag{5}$$

$$F_i^V = F(v_i^N)y_i + FP_i^V \tag{6}$$

Maritime carbon tax is levied based on CO_2 emissions. Therefore, the carbon tax can be expressed as $p_c\sum_{i=1}^{n}(\gamma F_i^L + \theta F_i^V)$ [45].

2.3.4. Methane Slip Cost

Methane slip from the ship's main engine is a critical issue faced by LNG dual-fuel powered vessels. The methane slip tax rate is $p_m = 30p_c$ [30]. Thus, the methane slip cost can be calculated as $p_m\sigma\sum_{i=1}^{n}[\frac{d_i^E}{v_i^E} + \frac{d_i^N}{v_i^N}(1 - y_i)]$.

2.3.5. Late Arrival Penalty

To improve the efficiency of liner services, time window constraints are imposed on arrival times. When a liner vessel arrives at a port late, a delay cost is incurred. Therefore, the late arrival penalty equals $\sum_{i=1}^{n}\varepsilon \max\{T_i^a - T_i^E, 0\}$ [46].

2.3.6. Model Formulation for LNG Dual-Fuel Powered Vessels

According to the analysis of various cost components presented above, this study constructs Model M1 to minimize the total cost Z_1 for a round voyage, such that

$$
\begin{aligned}
min\ Z_1 = kC_0 + \sum_{i=1}^{n}[p_i^L Q_i^L x_i^L + p_i^V Q_i^V x_i^V + C_g(x_i^L + x_i^V)] + p_c \sum_{i=1}^{n}(\gamma F_i^L + \theta F_i^V) \\
+ p_m \sigma \sum_{i=1}^{n}[\frac{d_i^E}{v_i^E} + \frac{d_i^N}{v_i^N}(1-y_i)] + \sum_{i=1}^{n} \varepsilon \max\{T_i^a - T_i^E, 0\}
\end{aligned} \tag{7}
$$

subject to

$$\sum_{i=1}^{n}(\frac{d_i^E}{v_i^E} + \frac{d_i^N}{v_i^N} + t_i) \le 168k \tag{8}$$

$$1 \le k \le k_{max} \tag{9}$$

$$\alpha H_L x_i^L \le Q_i^L \le H_L x_i^L, \forall i \in P_{LNG} \tag{10}$$

$$Q_i^L = 0, \forall i \in P_{NON} \tag{11}$$

$$\alpha H_V x_i^V \le Q_i^V \le H_V x_i^V, \forall i \in P \tag{12}$$

$$w_i^L \ge \alpha H_L, \forall i \in P \tag{13}$$

$$w_i^V \ge \alpha H_V, \forall i \in P \tag{14}$$

$$w_i^L + Q_i^L \le H_L, \forall i \in P_{LNG} \tag{15}$$

$$w_i^V + Q_i^V \le H_V, \forall i \in P \tag{16}$$

$$w_{i+1}^L = w_i^L + Q_i^L - \varphi F(v_i^E) - \varphi F(v_i^N)(1-y_i) - \sigma[\frac{d_i^E}{v_i^E} + \frac{d_i^N}{v_i^N}(1-y_i)], \forall i < n \tag{17}$$

$$w_{i+1}^V = w_i^V + Q_i^V - F(v_i^N)y_i - FP_i^V, \forall i < n \tag{18}$$

$$w_1^L = w_i^L + Q_i^L - \varphi F(v_i^E) - \varphi F(v_i^N)(1-y_i) - \sigma[\frac{d_i^E}{v_i^E} + \frac{d_i^N}{v_i^N}(1-y_i)], i = n \tag{19}$$

$$w_1^V = w_i^V + Q_i^V - F(v_i^N)y_i - FP_i^V, i = n \tag{20}$$

$$w_1^L = w_1^V = w_0 \tag{21}$$

$$T_1^a = 0 \tag{22}$$

$$T_{n+1}^a = T \tag{23}$$

$$T_{i+1}^a = T_i^a + t_i + \frac{d_i^E}{v_i^E} + \frac{d_i^N}{v_i^N}, \forall i \in P \tag{24}$$

$$v_{min} \le v_i^E \le v_i^N \le v_{max}, \forall i \in P \tag{25}$$

$$\sum_{i=1}^{n}(x_i^L + x_i^V) \le s \tag{26}$$

$$k \in Z^* \tag{27}$$

$$x_i^L, x_i^V, y_i \in \{0,1\}, \forall i \in P \tag{28}$$

$$Q_i^L, Q_i^V, w_i^L, w_i^V \ge 0, \forall i \in P \tag{29}$$

The objective function (7) is established to cut the total cost. Constraint (8) ensures compliance with the weekly service frequency. Constraint (9) limits the maximum number of allocated vessels. Constraint (10) specifies the bunkering amount restriction at ports equipped with LNG bunkering facilities. Constraint (11) indicates that the bunkering amount at ports without LNG bunkering facilities must be zero. Constraint (12) defines the VLSFO bunkering amount limit at ports. Constraints (13) and (14) enforce the safety inventory requirements for fuel upon vessel arrival at ports. Constraints (15) and (16) impose the maximum capacity restrictions for LNG and VLSFO fuel tanks, respectively. Constraints (17)–(20) enforce the fuel stock upon arrival at ports. Constraint (21) specifies the initial fuel inventory. Constraints (22)–(24) impose the vessel arrival time window constraints at ports. Constraint (25) imposes the speed restrictions. Constraint (26) imposes the maximum bunkering frequency limit. Constraint (27) shows that the number of liner vessels assigned to the route is a non-negative integer. Constraint (28) defines binary decision variables indicating whether fuel bunkering is conducted at ports and whether fuel switching is performed outside ECAs. Constraint (29) requires that fuel bunkering amounts and inventory levels be non-negative.

2.4. Fuel Bunkering Model with Fuel Price Discounts

2.4.1. Bunkering Cost with Fuel Price Discounts

The bunkering amounts of LNG and VLSFO at the ports of call are denoted as Q_i^L and Q_i^V, respectively. Taking into account the price discounts, the LNG and VLSFO bunkering costs C_i^L and C_i^V at the ports of call are shown as follows

$$C_i^L = \begin{cases} p_i^L Q_i^L, \ 0 < Q_i^L \leq B_1 \\ p_i^L B_1 + \lambda_1 p_i^L (Q_i^L - B_1), \ B_1 < Q_i^L \leq B_2 \\ p_i^L B_1 + \lambda_1 p_i^L (B_2 - B_1) + \lambda_2 p_i^L (Q_i^L - B_2), \ Q_i^L > B_2 \end{cases} \tag{30}$$

$$C_i^V = \begin{cases} p_i^V Q_i^V, \ 0 < Q_i^V \leq B_1 \\ p_i^V B_1 + \lambda_1 p_i^V (Q_i^V - B_1), \ B_1 < Q_i^V \leq B_2 \\ p_i^V B_1 + \lambda_1 p_i^V (B_2 - B_1) + \lambda_2 p_i^V (Q_i^V - B_2), \ Q_i^V > B_2 \end{cases} \tag{31}$$

where λ_1 is the price discount rate when the bunkering amount is in the interval (B_1, B_2], and λ_2 is the price discount rate when the bunkering amount exceeds B_2.

Furthermore, the total fixed cost for all bunkering operations $C_g(x_i^L + x_i^V)$ incurred during the fuel bunkering process must be taken into account. Consequently, the total bunkering cost for LNG dual-fuel powered vessels over the voyage route can be formulated as $\sum_{i=1}^{n} [C_i^L + C_i^V + C_g(x_i^L + x_i^V)]$.

2.4.2. Formulation of the Model with Fuel Price Discounts

Based on the bunkering cost analysis described above, an optimization Model M2 is formulated to reduce the total cost Z_2. Hence

$$\begin{aligned} \text{Min } Z_2 = \quad & kC_0 + \sum_{i=1}^{n} [C_i^L + C_i^V + C_g(x_i^L + x_i^V)] + p_c \sum_{i=1}^{n} (\gamma F_i^L + \theta F_i^V) \\ & + p_m \sigma \sum_{i=1}^{n} [\frac{d_i^E}{v_i^E} + \frac{d_i^N}{v_i^N}(1 - y_i)] + \sum_{i=1}^{n} \varepsilon \max\{T_i^a - T_i^E, 0\} \end{aligned} \tag{32}$$

The remaining constraints are the same as those in Model M1. Objective function (32) minimizes the total cost for LNG dual-fuel powered vessels on a round voyage considering fuel price discounts.

3. Linearization

This study constructs two mixed-integer nonlinear programming (MINLP) models. However, the models contain some nonlinear terms, which are relatively difficult to solve through CPLEX solver. In this section, auxiliary variables are introduced to reformulate the models as mixed-integer linear programming (MILP) models. The two MILP models are solved using MATLAB R2023a integrated with the YALMIP toolbox and the CPLEX 12.10.

3.1. Linearization of Nonlinear Terms

3.1.1. Linearization of Late Arrival Penalty Functions

In the model, the late arrival penalty is nonlinear, making it difficult to get the solutions. Thus, linearization of the late arrival penalty is required. Auxiliary variables μ_i are introduced, where $\mu_i = \max\{T_i^a - T_i^E, 0\}$, $i = 1, 2, \ldots, n$, to reformulate the original nonlinear terms as linear terms. Thus, the late arrival penalty functions are reformulated as

$$min\sum_{i=1}^{n} \varepsilon \max\left\{T_i^a - T_i^E, 0\right\} = \varepsilon\, min\sum_{i=1}^{n} \mu_i \tag{33}$$

subject to

$$\mu_i \geq T_i^a - T_i^E \tag{34}$$

$$\mu_i \geq 0 \tag{35}$$

3.1.2. Linearization of Fuel Consumption Functions

Equations (1), (2), (5) and (6) include nonlinear items. To solve the problem, nonlinear terms must be converted to linear terms [47]. Four steps are shown as follows:

Step 1. Auxiliary variables u_i^E and u_i^N are introduced, defined as $u_i^E = \frac{1}{v_i^E}$, $u_i^N = \frac{1}{v_i^N}$. Consequently, the speed range is transformed from $[v_{min}, v_{max}]$ to $[u_{min}, u_{max}]$, where $u_{min} = \frac{1}{v_{max}}$, $u_{max} = \frac{1}{v_{min}}$. Thereafter, the fuel consumption functions can be reformulated as

$$G(u_i^E) = F^M \varphi \frac{d_i^E (u_i^E)^{-2}}{{v_0}^3} \tag{36}$$

$$G_L(u_i^N) = F^M \varphi \frac{d_i^N (u_i^N)^{-2}}{{v_0}^3} \tag{37}$$

$$G_V(u_i^N) = F^M \frac{d_i^N (u_i^N)^{-2}}{{v_0}^3} \tag{38}$$

Step 2. Let $[u_{min}, u_{max}]$ be divided into X equal segments, and then $(X+1)$ division points can be obtained. The value at the *m-th* division point is denoted as u_{im}^E. Similarly, the value of u_{im}^N can be obtained.

$$u_{im}^E = u_{min} + (m-1)\frac{(u_{max} - u_{min})}{X} \tag{39}$$

$$u_{im}^N = u_{min} + (m-1)\frac{(u_{max} - u_{min})}{X} \tag{40}$$

Step 3. At the *m-th* division point, the fuel consumption amounts of LNG and VLSFO within and outside ECAs are $G(u_{im}^E)$, $G_L(u_{im}^N)$ and $G_V(u_{im}^N)$.

Step 4. For the ECA segment on voyage leg i, X piecewise linear functions can be derived from Step 3. To handle these X continuous piecewise functions, $(X+1)$ auxiliary continuous variables $\omega_{i1}^E, \omega_{i2}^E, \ldots, \omega_{i(X+1)}^E$ and X binary variables $\eta_{i1}^E, \eta_{i2}^E, \ldots, \eta_{iX}^E$ are introduced. The auxiliary continuous variables $\omega_{i1}^E, \omega_{i2}^E, \ldots, \omega_{i(X+1)}^E$ serve to achieve linearization of the fuel consumption functions, while the binary variables $\eta_{i1}^E, \eta_{i2}^E, \ldots, \eta_{iX}^E$ are used to ensure that u_i^E falls into exactly one interval. Consequently, the resulting linear constraints are formulated as follows

$$u_i^E = \omega_{i1}^E u_{i1}^E + \omega_{i2}^E u_{i2}^E + \cdots + \omega_{i(X+1)}^E u_{i(X+1)}^E \tag{41}$$

$$G(u_i^E) = \omega_{i1}^E G(u_{i1}^E) + \omega_{i2}^E G(u_{i2}^E) + \cdots + \omega_{i(X+1)}^E G(u_{i(X+1)}^E) \tag{42}$$

$$\omega_{i1}^E + \omega_{i2}^E + \cdots + \omega_{i(X+1)}^E = 1 \tag{43}$$

$$\omega_{im}^E \geq 0, \forall i \in R_E, m = 1, 2, \cdots, X+1 \tag{44}$$

$$\eta_{i1}^E + \eta_{i2}^E + \cdots + \eta_{iX}^E = 1 \tag{45}$$

$$\omega_{i1}^E \leq \eta_{i1}^E, \omega_{i2}^E \leq \eta_{i1}^E + \eta_{i2}^E, \cdots, \omega_{iX}^E \leq \eta_{i(X-1)}^E + \eta_{iX}^E, \omega_{i(X+1)}^E \leq \eta_{iX}^E \tag{46}$$

$$\eta_{im}^E \in \{0, 1\}, \forall i \in R_E, m = 1, 2, \cdots, X \tag{47}$$

Similarly, outside ECAs, the vessel can choose LNG or VLSFO as fuel. Thus, fuel consumption functions on leg i outside ECAs can be linearized separately.

3.1.3. Linearization of the Product Terms

In Model M1, there exist nonlinear forms involving the product terms between binary and non-negative continuous variables, such as $\varphi F(v_i^N)(1-y_i)$, $F(v_i^N)y_i$ and $\sigma \frac{d_i^N}{v_i^N}(1-y_i)$. Auxiliary variables z_i^1, z_i^2, and z_i^3 are introduced, where $z_i^1 = G_L(u_i^N)(1-y_i)$, $z_i^2 = G_V(u_i^N)y_i$ and $z_i^3 = H^N(1-y_i)$, with $H^N = \sigma d_i^N u_i^N$. The linearization of these nonlinear forms is achieved by adding the following constraints

$$z_i^1 \leq G_L(u_i^N), \forall i \in R_N \tag{48}$$

$$z_i^1 \geq G_L(u_i^N) - y_i M, \forall i \in R_N \tag{49}$$

$$z_i^1 \leq (1-y_i)M, \forall i \in R_N \tag{50}$$

$$z_i^2 \leq G_V(u_i^N), \forall i \in R_N \tag{51}$$

$$z_i^2 \geq G_V(u_i^N) - (1-y_i)M, \forall i \in R_N \tag{52}$$

$$z_i^2 \leq y_i M, \forall i \in R_N \tag{53}$$

$$z_i^3 \leq H^N, \forall i \in R_N \tag{54}$$

$$z_i^3 \geq H^N - y_i M, \forall i \in R_N \tag{55}$$

$$z_i^3 \leq (1-y_i)M, \forall i \in R_N \tag{56}$$

$$z_i^1, z_i^2, z_i^3 \geq 0, \forall i \in R_N \tag{57}$$

where M is fixed and large enough.

3.1.4. Linearization of Piecewise Functions for Fuel Bunkering Costs

To determine the fuel bunkering strategy for dual-fuel vessels, the fuel bunkering costs need to be linearized [48]. During the fuel bunkering process at ports, the unit fuel price decreases with the increase in bunkering amount to reflect the scale discount effect. Given that the fuel price demonstrates piecewise function characteristics, linearization processing is necessary. Specifically, Equations (30) and (31) are non-smooth functions that require linearization. First, the LNG bunkering cost C_i^L is linearized by introducing four continuous variables τ_i^1, τ_i^2, τ_i^3, τ_i^4 to achieve function linearization, and three binary variables ϱ_i^1, ϱ_i^2, ϱ_i^3 are introduced to constrain the values of these four continuous variables. Equation (30) is transformed as

$$\begin{aligned} C_i^L = \quad & \tau_i^1 0 + \tau_i^2 p_i^L B_1 + \tau_i^3 [p_i^L B_1 + \lambda_1 p_i^L (B_2 - B_1)] \\ & + \tau_i^4 [p_i^L B_1 + \lambda_1 p_i^L (B_2 - B_1) + \lambda_2 p_i^L (H_L - B_2)], \ \forall i \in P_{LNG} \end{aligned} \tag{58}$$

$$Q_i^L = \tau_i^1 0 + \tau_i^2 B_1 + \tau_i^3 B_2 + \tau_i^4 H_L,\ \forall i \in P_{LNG} \tag{59}$$

$$\tau_i^1 \leq \varrho_i^1,\ \forall i \in P_{LNG} \tag{60}$$

$$\tau_i^j \leq \varrho_i^{j-1} + \varrho_i^j,\ j = 2,\ 3,\ \forall i \in P_{LNG} \tag{61}$$

$$\tau_i^4 \leq \varrho_i^3,\ \forall i \in P_{LNG} \tag{62}$$

$$\tau_i^1 + \tau_i^2 + \tau_i^3 + \tau_i^4 = x_i^L, \forall i \in P_{LNG} \tag{63}$$

$$\varrho_i^1 + \varrho_i^2 + \varrho_i^3 = x_i^L, \forall i \in P_{LNG} \tag{64}$$

$$\tau_i^j \geq 0,\ j = 1,\ 2,\ 3,\ 4,\ \forall i \in P_{LNG} \tag{65}$$

$$\varrho_i^j \in \{0,\ 1\},\ j = 1,\ 2,\ 3,\ \forall i \in P_{LNG} \tag{66}$$

Subsequently, the VLSFO bunkering cost C_i^V undergoes linearization processing, whereby four auxiliary continuous variables $\tilde{\tau}_i^1, \tilde{\tau}_i^2, \tilde{\tau}_i^3, \tilde{\tau}_i^4$ are introduced to achieve function linearization, and three binary variables $\tilde{\varrho}_i^1, \tilde{\varrho}_i^2, \tilde{\varrho}_i^3$ are introduced to constrain the values of these four continuous variables. Equation (31) is reformulated as

$$\begin{aligned} C_i^V = &\ \tilde{\tau}_i^1 0 + \tilde{\tau}_i^2 p_i^V B_1 + \tilde{\tau}_i^3 [p_i^V B_1 + \lambda_1 p_i^V (B_2 - B_1)] \\ &+ \tilde{\tau}_i^4 [p_i^V B_1 + \lambda_1 p_i^V (B_2 - B_1) + \lambda_2 p_i^V (H_V - B_2)],\ \forall i \in P \end{aligned} \tag{67}$$

$$Q_i^V = \tilde{\tau}_i^1 0 + \tilde{\tau}_i^2 B_1 + \tilde{\tau}_i^3 B_2 + \tilde{\tau}_i^4 H_V,\ \forall i \in P \tag{68}$$

$$\tilde{\tau}_i^1 \leq \tilde{\varrho}_i^1,\ \forall i \in P \tag{69}$$

$$\tilde{\tau}_i^j \leq \tilde{\varrho}_i^{j-1} + \tilde{\varrho}_i^j,\ j = 2,\ 3,\ \forall i \in P \tag{70}$$

$$\tilde{\tau}_i^4 \leq \tilde{\varrho}_i^3,\ \forall i \in P \tag{71}$$

$$\tilde{\tau}_i^1 + \tilde{\tau}_i^2 + \tilde{\tau}_i^3 + \tilde{\tau}_i^4 = x_i^V,\ \forall i \in P \tag{72}$$

$$\tilde{\varrho}_i^1 + \tilde{\varrho}_i^2 + \tilde{\varrho}_i^3 = x_i^V, \forall i \in P \tag{73}$$

$$\tilde{\tau}_i^j \geq 0,\ j = 1,\ 2,\ 3,\ 4,\ \forall i \in P \tag{74}$$

$$\tilde{\varrho}_i^j \in \{0,\ 1\},\ j = 1,\ 2,\ 3,\ \forall i \in P \tag{75}$$

3.2. Model Transformation

3.2.1. Transformation of the Fuel Bunkering Model

The auxiliary variables are introduced to obtain the solutions of Model M1. The main engine fuel consumption amounts $\varphi F(v_i^E)$, $\varphi F(v_i^N)(1 - y_i)$ and $F(v_i^N) y_i$ are transformed into linear expressions, as follows

$$\varphi F(v_i^E) = G(u_i^E) \tag{76}$$

$$\varphi F(v_i^N)(1 - y_i) = z_i^1 \tag{77}$$

$$F(v_i^N) y_i = z_i^2 \tag{78}$$

By introducing auxiliary variables, Model M1 is transformed into Model M3, defined as follows

$$\begin{aligned} min\ Z_3 = kC_0 + \sum_{i=1}^{n} [p_i^L Q_i^L x_i^L + p_i^V Q_i^V x_i^V + C_g(x_i^L + x_i^V)] + p_c \sum_{i=1}^{n} (\gamma F_i^L + \theta F_i^V) \\ + p_m \sigma \sum_{i=1}^{n} [d_i^E u_i^E + d_i^N u_i^N (1 - y_i)] + \varepsilon \sum_{i=1}^{n} \mu_i \end{aligned} \quad (79)$$

subject to

$$\sum_{i=1}^{n} (d_i^E u_i^E + d_i^N u_i^N + t_i) \leq 168k \quad (80)$$

$$w_{i+1}^L = w_i^L + Q_i^L - G(u_i^E) - z_i^1 - \sigma d_i^E u_i^E - z_i^3, \forall i < n \quad (81)$$

$$w_{i+1}^V = w_i^V + Q_i^V - z_i^2 - FP_i^V, \forall i < n \quad (82)$$

$$w_1^L = w_i^L + Q_i^L - G(u_i^E) - z_i^1 - \sigma d_i^E u_i^E - z_i^3, i = n \quad (83)$$

$$w_1^V = w_i^V + Q_i^V - z_i^2 - FP_i^V, i = n \quad (84)$$

$$T_{i+1}^a = T_i^a + t_i + d_i^E u_i^E + d_i^N u_i^N, \forall i \in P \quad (85)$$

$$u_{min} \leq u_i^N \leq u_i^E \leq u_{max}, \forall i \in P \quad (86)$$

Model M3 retains some constraints from Model M1, specifically including Equations (9)–(16), (21)–(23) and (26)–(29). The nonlinear constraints in Model M1, namely Equations (8), (17)–(20), (24) and (25), are transformed into linear constraints Equations (80)–(86). The remaining constraints are newly added linear constraints after introducing auxiliary variables, including Equations (33)–(57). Furthermore, the linearization constraints for fuel consumption functions outside ECAs should be included.

3.2.2. Transformation of the Model with Fuel Price Discounts

Through the linearization of the bunkering cost in Model M2, the nonlinear terms have been converted into linear terms. Therefore, Model M2 is transformed into Model M4, defined as follows

$$\begin{aligned} min\ Z_4 = kC_0 + \sum_{i=1}^{n} [C_i^L + C_i^V + C_g(x_i^L + x_i^V)] + p_c \sum_{i=1}^{n} (\gamma F_i^L + \theta F_i^V) \\ + p_m \sigma \sum_{i=1}^{n} [d_i^E u_i^E + d_i^N u_i^N (1 - y_i)] + \varepsilon \sum_{i=1}^{n} \mu_i \end{aligned} \quad (87)$$

Equations (58)–(75) are the newly added constraints for the linearization of bunkering costs, and the remaining constraints are the same as those in Model M3.

4. Case Study and Sensitivity Analyses

4.1. Relevant Data for the Route and Models

A case study will be conducted on the ship *CMA CGM Jacques Saadé*, which serves the Far East–Northwest Europe route. Based on the route information collected from the *CMA CGM* and HiFleet website, the actual operational route has been supplemented. On the basis of the original route, port calls at Port Said, Yantian, and Shanghai Yangshan ports have been included. The westbound leg of the route departs from Qingdao, China, passes through Shanghai Yangshan Port, Ningbo, Yantian, and Singapore, and arrives at Le Havre. The eastbound leg departs from Le Havre, passes through Rotterdam, Hamburg, Antwerp, Tangier Med Port, Port Said, Port Klang, Yantian, and Shanghai Yangshan ports, before finally returning to Qingdao. The route map was generated using Adobe Illustrator, based on the HiFleet website map, as shown in Figure 2. This study assumes that, except for Tangier Med, which has no LNG refueling capacity, all other ports can refuel LNG in the future.

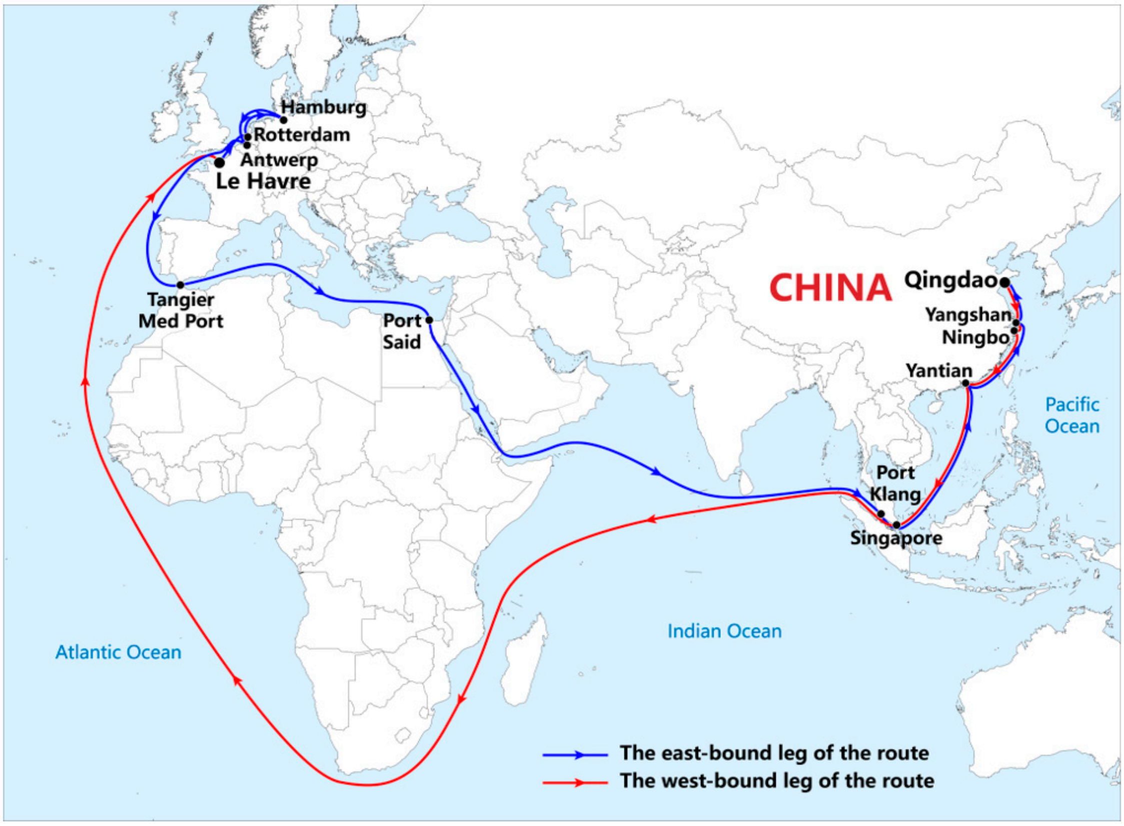

Figure 2. The shipping route and ports.

According to the data collected from Clarksons Intelligence Network for the container liner ship *CMA CGM Jacques Saadé*, the loading capacity is 23,112 TEU. The other parameter values are listed in Table 2.

The number of segments for the fuel consumption functions is 100. Route data, including port calls, berthing time and distance, were collected from the HiFleet website. According to the data on fuel prices at some ports, the average price of LNG in 2025 is 708 USD/ton, and the average price of VLSFO is 513 USD/ton. Meanwhile, fuel prices at various ports were collected from the Oil Monster website. However, since this platform only provides fuel price data for some ports, normally distributed data was generated for missing data, where the mean equals the annual average fuel price and the standard deviation is taken as 20 [31]. The related data are shown in Table 3.

Table 2. Parameter values for the two models.

Parameter	Value	Parameter	Value	Parameter	Value
T	2520	α	10%	SF^M	206
v_0	18.50	β	0.02	EL^M	0.8
v_{max}	22	γ	2.75	PS^M	63,840
v_{min}	10	θ	3.151	C_0	225,000
C_g	1000	φ	0.81	B_1	1000
H_L	8500	σ	0.11	B_2	2000
H_V	2300	ε	1000	λ_1	0.95
s	6	k_{max}	15	λ_2	0.90
p_c	70	p_m	2100	w_0	1000

Table 3. Route-related data.

No.	Port	Distance, nm		Berthing Time, h	Arrival Time, h	Price, USD/ton	
		Outside ECAs	Inside ECAs			LNG	VLSFO
1	Qingdao	395	0	31	0	692	530.50
2	Shanghai Yangshan	55	0	42	81	668	524.75
3	Ningbo	701	0	45	134	701	611
4	Yantian	1464	0	35	253	696	628
5	Singapore	11,438	219	40	376	606	451
6	Le Havre	0	247	68	1051	711	485
7	Rotterdam	0	304	84	1143	643	430
8	Hamburg	0	396	48	1251	688	485
9	Antwerp	987	455	53	1334	697	419
10	Tangier Med	0	1949	37	1518	—	595
11	Port Said	4902	18	10	1698	728	472
12	Klang	1679	0	106	2099	708	588
13	Yantian	760	0	37	2301	696	628
14	Shanghai Yangshan	396	0	37	2428	668	524.75
15	Qingdao	—	—	—	2520	692	530.50

4.2. Results

According to the collected data above, we get the solutions for Model M3 using MATLAB R2023a. For the round-trip voyage, 15 LNG dual-fuel powered ships are required, with a minimum total cost of USD 10,020,546. The total cost consists of LNG bunkering cost of USD 3,122,267, VLSFO bunkering cost of USD 1,462,700, carbon tax of USD 1,681,894, methane slip cost of USD 230,385 and late arrival penalty of USD 148,300. After retaining two decimal places, the proportion of each cost item can be obtained, as shown in Figure 3.

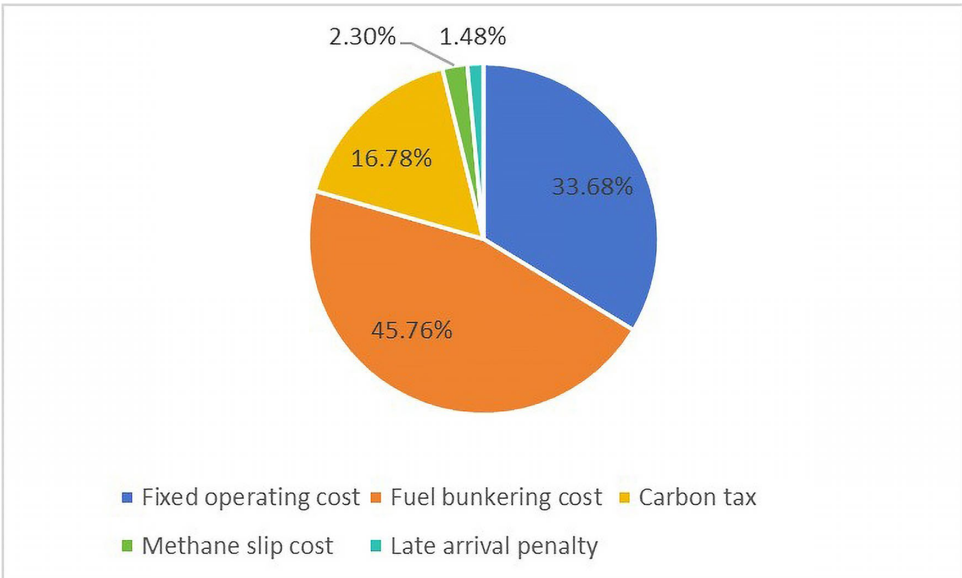

Figure 3. The proportion of each cost item in Model M3.

Table 4 details the planned speeds for each leg, arrival times, whether VLSFO is used outside these ECAs, and the fuel bunkering amount at each port. As shown in Table 4, the planned speeds for the liner vessel within the ECAs from Singapore to Port Said are 16.03, 15.49, 14.86, 14.07, 12.97, 13.25 and 12.53 knots, respectively. Similarly, the planned speeds outside these ECAs can also be obtained. However, the latest arrival times are exceeded at the Le Havre, Rotterdam, Hamburg, Antwerp, Yantian and Shanghai Yangshan ports. This is because, considering the carbon tax and the bunkering fuel cost required for subsequent voyage legs, the container vessel compromised on the arrival time at these ports. Table 4 indicates that the vessel engaged in fuel tankering in Singapore, loading 5150.61 tons of LNG, to sustain operations across the long trans-oceanic leg between Singapore and Antwerp. It implies that on long legs, the model favors ensuring fuel feasibility rather than achieving speed optimality. It also bunkers VLSFO at Shanghai Yangshan Port, Antwerp, Port Said, and Shanghai Yangshan Port, with amounts of 230.00 tons, 2070.00 tons, 287.24 tons and 638.59 tons, respectively. Among these ports, Antwerp has the lowest VLSFO fuel price, with a bunkering amount of up to 2070.00 tons.

Table 4. The solution derived from Model M3.

No	Port	Speed, kn		Arrival Time, h	y_i	Bunkering Amount, ton	
		Outside ECAs	Inside ECAs			LNG	VLSFO
1	Qingdao	16.18	—	0	0	0	0
2	Shanghai Yangshan	15.76	—	55.42	1	0	230.00
3	Ningbo	15.62	—	100.91	1	0	0
4	Yantian	15.75	—	190.77	1	0	0
5	Singapore	16.08	16.03	318.72	0	5150.61	0
6	Le Havre	—	15.49	1083.52	—	0	0
7	Rotterdam	—	14.86	1167.47	—	0	0
8	Hamburg	—	14.07	1271.92	—	0	0
9	Antwerp	12.97	12.97	1348.07	1	0	2070.00
10	Tangier	—	13.25	1512.23	—	—	0
11	Port Said	12.53	12.53	1696.29	1	0	287.24
12	Klang	12.36	—	2099.00	1	0	0
13	Yantian	11.41	—	2340.85	1	0	0
14	Shanghai Yangshan	10.28	—	2444.48	1	0	638.59
15	Qingdao	—	—	2520	—	—	—

Model M4 considers the effect of fuel price discounts on decision-making. The results show that 15 ships are required to complete the weekly liner transportation service, with a minimum total cost of USD 9,748,737. The total cost consists of the LNG bunkering cost of USD 3,367,085, VLSFO bunkering cost of USD 966,140, carbon tax of USD 1,636,540, methane slip cost of USD 291,862 and late arrival penalty of USD 112,110. After retaining two decimal places, the proportion of each cost component is illustrated in Figure 4.

The planned speeds for each leg, arrival times, whether VLSFO is used outside these ECAs, and the fuel bunkering amount at each port are listed in Table 5. Comparing Tables 4 and 5, it was found that introducing fuel price discounts increases the LNG bunkering volume from 5150.61 tons to 6005.11 tons, even though Singapore remains the same refueling port in both scenarios. For VLSFO, without fuel price discounts, the ship refueled four times, with 230.00, 2070.00, 287.24 and 638.59 tons, respectively, at the Shanghai Yangshan, Antwerp, Said, and Shanghai Yangshan ports. However, if fuel price discounts are introduced, this vessel makes only two VLSFO bunkering stops, driven by the increased refueling amount of LNG. The results indicate that fuel price discounts have a significant impact on the selection of the LNG refueling volumes and VLSFO refueling ports.

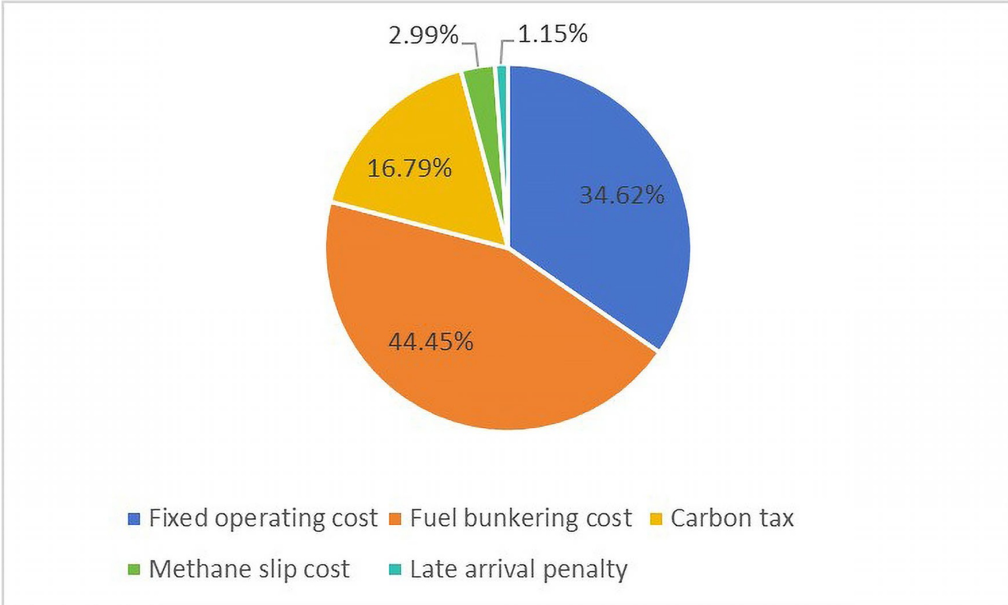

Figure 4. The proportion of each cost component to the total operational cost in Model M4.

Table 5. The solution derived from Model M4.

No.	Port	Speed, kn		Arrival Time, h	y_i	Bunkering Amount, ton	
		Outside ECAs	Inside ECAs			LNG	VLSFO
1	Qingdao	16.32	—	0	0	0	0
2	Shanghai Yangshan	15.76	—	55.20	1	0	230.00
3	Ningbo	15.76	—	100.69	1	0	0
4	Yantian	15.66	—	190.17	1	0	0
5	Singapore	16.28	16.18	318.67	0	6005.11	0
6	Le Havre	—	15.62	1074.78	—	0	0
7	Rotterdam	—	14.86	1158.59	—	0	0
8	Hamburg	—	14.07	1263.04	—	0	0
9	Antwerp	13.25	13.25	1339.19	0	0	2070.00
10	Tangier	—	13.25	1501.00	—	—	0
11	Port Said	12.18	12.18	1685.06	1	0	0
12	Klang	12.52	—	2099.00	0	0	0
13	Yantian	11.29	—	2339.11	0	0	0
14	Shanghai Yangshan	10.00	—	2443.40	1	0	0
15	Qingdao	—	—	2520	—	—	—

As shown in Table 6, considering fuel price discounts, compared with M3, the total operational cost decreases by USD 271,809, and the fuel bunkering cost decreases by USD 251,742. Specifically, the LNG bunkering cost increases by USD 244,818, and the VLSFO bunkering cost decreases by USD 496,560. Overall, the total cost, fuel bunkering cost and carbon tax decreased significantly. Conversely, the LNG bunkering cost and methane slip cost increased substantially.

Table 6. Cost comparison of liner shipping service between the two models, USD.

Cost	Model M3	Model M4	Absolute Change	Relative Percent Change
Total operational cost	10,020,546	9,748,737	−271,809	−2.71%
Fuel bunkering cost	4,584,967	4,333,225	−251,742	−5.49%

Table 6. *Cont.*

Cost	Model M3	Model M4	Absolute Change	Relative Percent Change
LNG bunkering cost	3,122,267	3,367,085	244,818	7.84%
VLSFO bunkering cost	1,462,700	966,140	−496,560	−33.95%
Carbon tax	1,681,894	1,636,540	−45,354	−2.70%
Methane slip cost	230,385	291,862	61,477	26.68%
Late arrival penalty	148,300	112,110	−36,190	−24.40%

4.3. Sensitivity Analyses

4.3.1. Fuel Price Difference

Fuel prices are often influenced by a variety of factors and exhibit dynamic fluctuations over time. The study shows the impact of the price difference δ_i between LNG and VLSFO on shipping companies' operational decisions, $\delta_i = p_i^L - p_i^V$. In the sensitivity analysis, it is assumed that the LNG prices change while other parameters and VLSFO prices are fixed. The changes of cost, fuel bunkering amount and planned speed are analyzed when the price difference is set to 100, 200, 300 and 400 USD/ton, respectively. The results are shown in Figures 5–7.

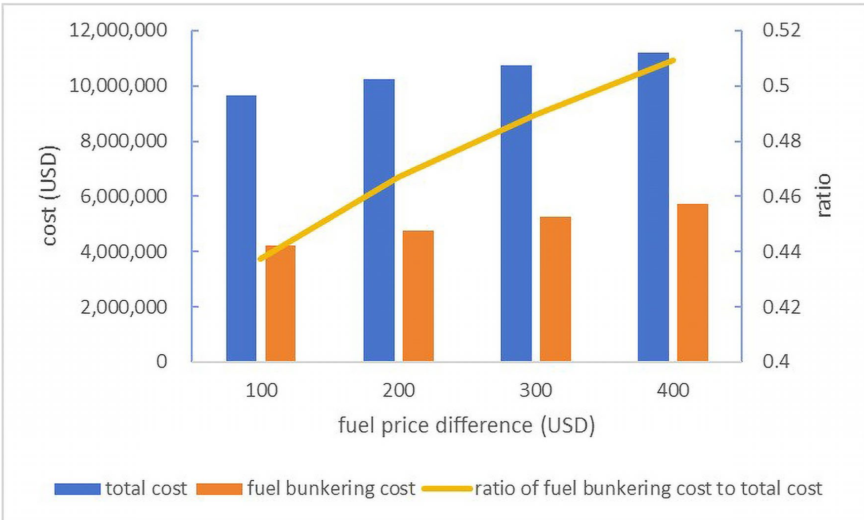

Figure 5. Costs under four fuel price differences.

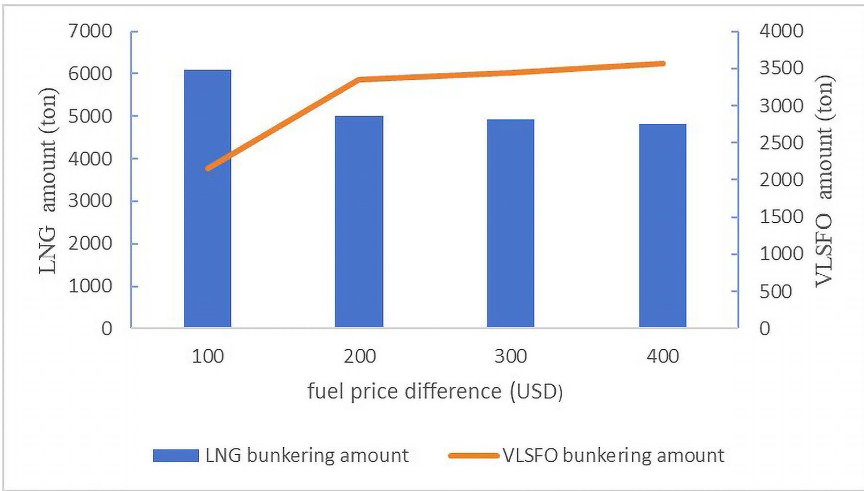

Figure 6. Fuel bunkering amounts under four fuel price differences.

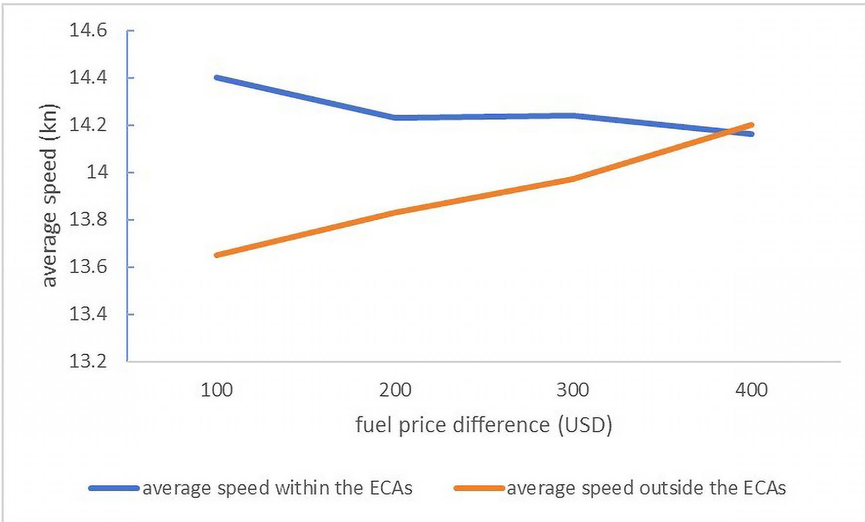

Figure 7. Average speeds under four fuel price differences.

Figure 5 shows that with the increase in the price difference, the bunkering cost, the total cost and the ratio between them show an increasing trend. The ratio of fuel bunkering cost to the total cost increases rapidly, rising from 43.72% to 50.92%. The results show that when the fuel price difference is significant, shipping companies should optimize the fuel bunkering strategy of ships, particularly by making timely estimations of changes in LNG and VLSFO bunkering costs.

Figure 6 provides the fuel bunkering amounts of LNG and VLSFO under four fuel price differences. When the fuel price difference is 100 USD/ton, the LNG bunkering amount is the highest, while the VLSFO refueling volume is the lowest. When the fuel price difference is 200, the LNG bunkering volume decreases by approximately 1000 tons. As the fuel price difference continues to increase, LNG bunkering volumes have gradually decreased, while VLSFO bunkering amounts gradually increase, reaching a peak of 3563.12 tons. Shipping companies should adjust the fuel bunkering volumes timely and closely monitor VLSFO inventory levels to ensure normal navigation.

Figure 7 shows the changes of average speeds inside and outside these ECAs. With the increase in fuel price difference, the average speed within these ECAs gradually decreases, while the average speed outside ECAs gradually increases. This is because the price of LNG has risen, making the vessel slow down within ECAs, thereby lowering the fuel costs and complying with emissions regulations. Due to the penalty for delays, the average speed outside ECAs will increase.

4.3.2. Carbon Tax Rate

Carbon tax policies vary across different regions and there are significant differences in carbon tax rates. According to data released by the World Bank Group, the carbon tax rate levied in 2025 ranges from 0.1 USD/ton to 158.8 USD/ton. Therefore, we set the carbon tax rate to vary between 10 USD/ton and 160 USD/ton. Subsequently, this study analyzes the impact of carbon tax rate on vessel operational decisions. The results are shown in Figures 8 and 9.

Figure 8 shows the changes in total costs, carbon tax costs and carbon emissions under different carbon tax rates. As the carbon tax rate gradually increases, both the total cost and the carbon tax are rising. The carbon tax rises from USD 237,392.17 to USD 3,811,557.89, with a growth rate of 1505.60%. When the carbon tax rate is low, carbon emissions increase initially. When $p_c = 40$ USD/ton, the total carbon emissions are the highest. As the carbon tax rate continues to increase, the total carbon emissions first decrease rapidly and then decrease slowly. The results imply that carbon emissions of ships can be effectively reduced only when the carbon tax rate reaches a threshold, but it also increases the operational costs of ships.

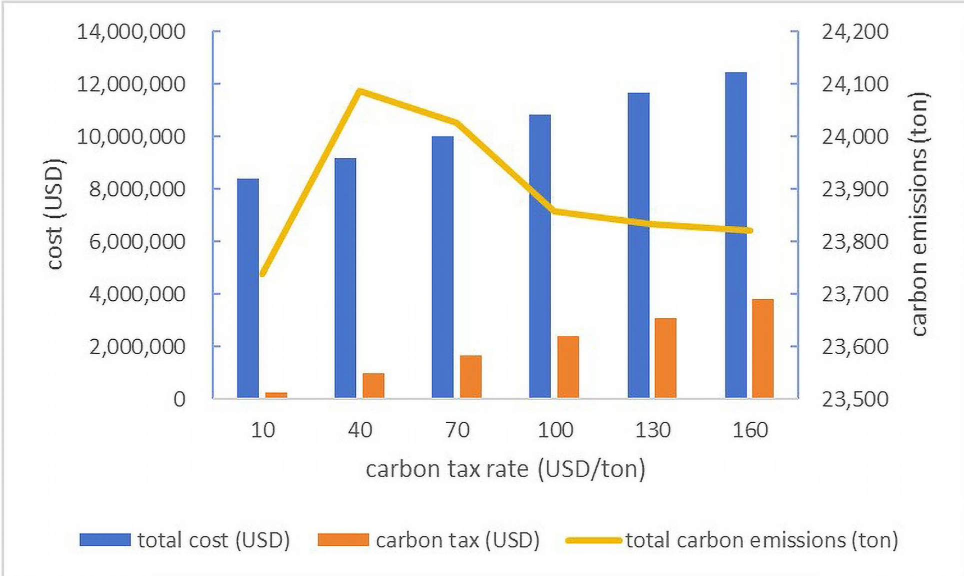

Figure 8. Costs and carbon emissions under different carbon tax rates.

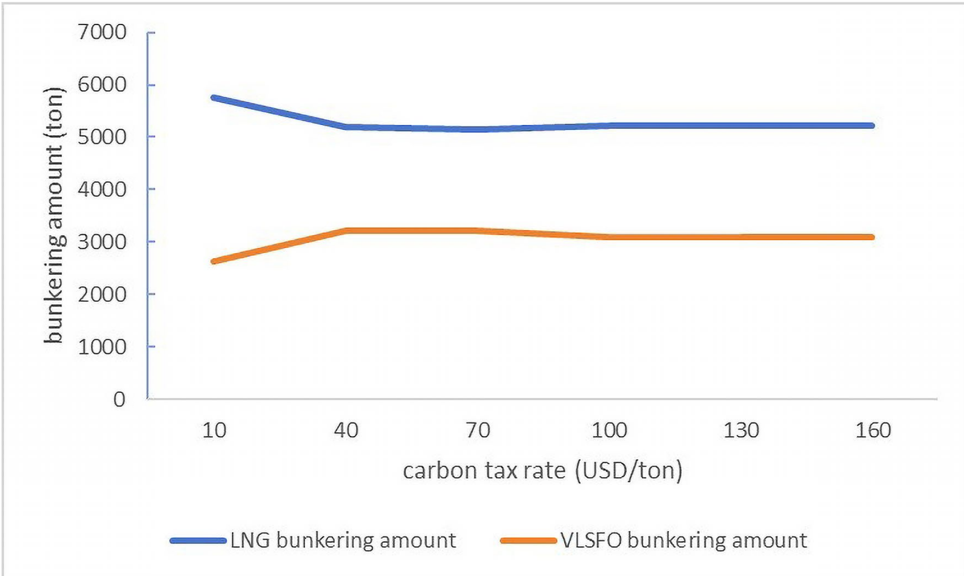

Figure 9. Fuel bunkering amounts under different carbon tax rates.

Figure 9 shows the impact of carbon tax rate on fuel bunkering amounts. Overall, the LNG bunkering amount initially declines rapidly and then stabilizes at approximately 5200 tons, while the VLSFO bunkering volume increases initially and finally stabilizes at 3100 tons. When $p_c = 10$ USD/ton and $p_m = 300$ USD/ton, carbon and methane taxes are relatively low, resulting in a higher LNG refueling amount. When $p_c = 40$ USD/ton, the LNG bunkering volume is significantly reduced by about 580 tons, and VLSFO increases by about 600 tons.

4.3.3. Methane Slip Rate

Methane slip rate is influenced by the type of ship engines, operating conditions and post-treatment equipment. Thus, while keeping other parameters constant, we investigate the impact of methane slip rate on operational decisions by varying it from 0.03 to 0.18. The results are shown in Figures 10 and 11.

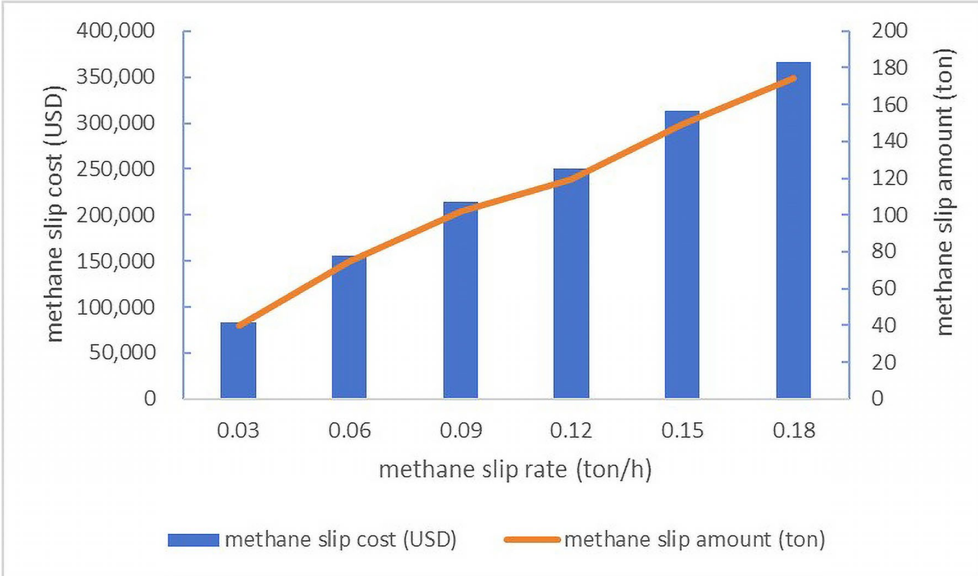

Figure 10. Methane slip costs and amounts under different methane slip rates.

Figure 10 illustrates how methane slip cost and methane slip amount vary under different methane slip rates. With the increase in methane slip rate, methane slip cost and methane slip amount show an increasing trend. The methane slip amount increases from 39.75 tons to 174.47 tons, and the methane slip cost increases by USD 283,302.12.

Figure 11 shows the variations in fuel bunkering amount and total carbon emissions under different methane slip rates. As the rate increases, the bunkering amount of LNG tends to decrease, while the VLSFO bunkering amount shows an upward trend. When $\sigma > 0.12$ ton/h, the total carbon emissions significantly increase. Relevant authorities should impose strict regulations on ship engines that cause high methane slip rates to ensure the effectiveness of ship emission reduction policies.

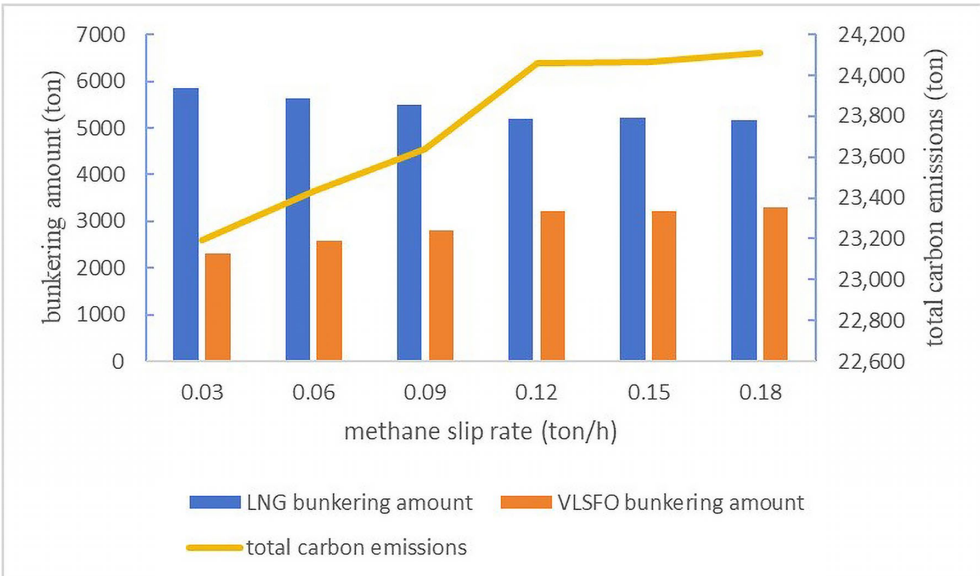

Figure 11. Fuel bunkering amounts under different methane slip rates.

5. Conclusions

The shipping industry supports the majority of global trade, but the associated severe air pollution problems cannot be overlooked. The research constructs a basic optimization model and an improved model that accounts for fuel price discounts. The objective is to minimize the total costs while meeting emission regulations. The primary work, conclusions and key insights are as follows

Firstly, this research integrates factors including methane slip, carbon tax, ECA policy, fuel price discounts and late arrival penalty into the modeling framework. To obtain the solutions, several nonlinear terms are linearized.

Secondly, a case study is conducted with the liner vessel *CMA CGM Jacques Saadé* navigating between the Northwest and Far East Europe. The bunkering amounts of LNG and VLSFO were calculated, the refueling ports for these two fuels were identified, and the vessel's planned speeds were determined.

Finally, the sensitivity of important parameters is analyzed. The results demonstrate that both fuel price discounts and fuel price differences have substantial effects on operational costs, carbon tax, bunkering amounts of different fuels, bunkering ports and planned speeds. When fuel price differences are excessively high, liner enterprises should adjust bunkering amounts and planned speeds promptly within and outside these ECAs. Only when the carbon tax rate reaches a specific value will the carbon tax policy exert a significant influence on reducing carbon emissions. At high carbon tax rates, the carbon emissions reduction rate slows down, and the marginal benefits of emission reductions decrease, but the total cost continues to rise. Moreover, the methane slip rate has a substantial impact on bunkering amounts and total carbon emissions. The results suggest that regulatory authorities should impose stringent limits on ship engines that exhibit high methane slip rates, so as to guarantee the effectiveness of emission reduction policies.

However, the effects of fuel switching time, ECA boundaries and co-reductions in multiple pollutants are not included in this study. In future studies, these factors can be taken into account. A sensitivity analysis of time window constraints is also recommended. Emerging technologies, including machine learning and artificial intelligence, offer great opportunities for data processing. Besides LNG, which is mentioned in this study, biomethane, methanol and fuel cells are also recognized as important research hotspots.

Author Contributions: Q.W.: Writing—original draft, Conceptualization, Methodology, Validation, Software, Funding acquisition, Formal analysis. S.L.: Writing—original draft, Validation, Visualization, Software. W.H.: Writing—review and editing, Validation. All authors have read and agreed to the published version of the manuscript.

Funding: This research received no external funding.

Data Availability Statement: All data are contained within the article.

Acknowledgments: The authors thank the editors and reviewers for their valuable comments.

Conflicts of Interest: The authors declare no conflicts of interest.

References

1. Ozbiltekin-Pala, M.; Kazancoglu, Y.; Karamperidis, S.; Ram, M. Managing the risks against carbon neutralization for green maritime transport. *J. Clean. Prod.* **2024**, *457*, 142478. [CrossRef]
2. Tadros, M.; Ventura, M.; Soares, C.G. Review of current regulations, available technologies, and future trends in the green shipping industry. *Ocean Eng.* **2023**, *280*, 114670. [CrossRef]
3. Deng, S.; Mi, Z. A review on carbon emissions of global shipping. *Mar. Dev.* **2023**, *1*, 4. [CrossRef]
4. Wang, Z.; Zhang, H.; Gan, X. Research on solution of ship low sulphur fuel based on IMO sulphur limitation regulation. *IOP Conf. Ser. Earth Environ. Sci. IOP Publ.* **2019**, *401*, 012012. [CrossRef]

5. Deng, J.; Wang, X.; Wei, Z.; Wang, L.; Wang, C.; Chen, Z. A review of NOx and SOx emission reduction technologies for marine diesel engines and the potential evaluation of liquefied natural gas fuelled vessels. *Sci. Total Environ.* **2021**, *766*, 144319. [CrossRef]
6. Kouzelis, K.; Frouws, K.; Van Hassel, E. Maritime fuels of the future: What is the impact of alternative fuels on the optimal economic speed of large container vessels. *J. Shipp. Trade.* **2022**, *7*, 23. [CrossRef]
7. Li, Z.; Zhang, H.; Zhang, J.; Wu, B. Joint Optimization of route and speed for methanol dual-fuel powered ships based on improved genetic algorithm. *Big Data Cogn. Comput.* **2025**, *9*, 90. [CrossRef]
8. Wu, Y.; Guo, H.; Qi, J.; Wang, S.; Zhen, L. Ship refueling optimization for dual-fuel ships considering carbon intensity indicator rating limit and uncertain fuel prices. *Multimodal Transp.* **2024**, *3*, 100138. [CrossRef]
9. Fragkou, E.; Tsegas, G.; Alyuz, U.; Hänninen, R.; Moldanova, J.; Jutterström, S.; Ntziachristos, L. Assessing the efficiency of different mitigation strategies to reduce shipping related air pollution levels and exposure in the Mediterranean coastal region–An ensemble modelling approach. *Atmos. Environ.* **2025**, *360*, 121347. [CrossRef]
10. Zis, T.P.V.; Psaraftis, H.N.; Tillig, F.; Ringsberg, J.W. Decarbonizing maritime transport: A Ro-Pax case study. *Res. Transp. Bus. Manag.* **2020**, *37*, 100565. [CrossRef]
11. Bouman, E.A.; Lindstad, E.; Rialland, A.I.; Strømman, A.H. State-of-the-art technologies, measures, and potential for reducing GHG emissions from shipping–A review. *Transp. Res. Part D Transp. Environ.* **2017**, *52*, 408–421. [CrossRef]
12. Issa, M.; Ilinca, A.; Martini, F. Ship energy efficiency and maritime sector initiatives to reduce carbon emissions. *Energies* **2022**, *15*, 7910. [CrossRef]
13. Dettner, F.; Hilpert, S. Modelling CO_2 emissions and mitigation potential of Northern European shipping. *Transp. Res. Part D Transp. Environ.* **2023**, *119*, 103745. [CrossRef]
14. Krantz, G.; Moretti, C.; Brandão, M.; Hedenqvist, M.; Nilsson, F. Assessing the environmental impact of eight alternative fuels in international shipping: A comparison of marginal vs. average emissions. *Environments* **2023**, *10*, 155. [CrossRef]
15. Tu, H.; Liu, Z.; Zhang, Y. Study on cost-effective performance of alternative fuels and energy efficiency measures for shipping decarbonization. *J. Mar. Sci. Eng.* **2024**, *12*, 743. [CrossRef]
16. Sagin, S.; Haichenia, O.; Karianskyi, S.; Kuropyatnyk, O.; Razinkin, R.; Sagin, A.; Volkov, O. Improving green shipping by using alternative fuels in ship diesel engines. *J. Mar. Sci. Eng.* **2025**, *13*, 589. [CrossRef]
17. Milojević, S.; Stopka, O.; Orynycz, O.; Tucki, K.; Šarkan, B.; Savić, S. Exploitation and maintenance of biomethane-powered truck and bus fleets to assure safety and mitigation of greenhouse gas emissions. *Energies* **2025**, *18*, 2218. [CrossRef]
18. Petrychenko, O.; Levinskyi, M. Trends and preconditions for widespread adoption of liquefied natural gas in maritime transport. *Transp. Syst. Technol.* **2024**, 21–36. [CrossRef]
19. Zou, Q.; Yi, C.; Wang, K.; Yin, X.; Zhang, Y. Global LNG market: Supply-demand and economic analysis. *IOP Conf. Ser. Earth Environ. Sci. IOP Publ.* **2022**, *983*, 012051. [CrossRef]
20. Wei, M.; Zhou, Y.; Gao, J.; Wang, Y.; Pan, F. Review of world shipping market in 2023 and prospect in 2024. *Ship Boat.* **2024**, *35*, 1–18.
21. He, P.; Wu, L.; Jin, J.G.; Zhou, S.; Schulte, F. Distributionally robust optimization of sailing speed, bunkering, and fuel switching for dual-fuel liner services. *Transp. Res. Part C Emerg. Technol.* **2026**, *184*, 105528. [CrossRef]
22. Gu, Y.; Wang, Y.; Iris, Ç. Integrated green technology adoption, ship speed optimization and slot management for shipping alliance under emission limits and uncertain fuel prices. *J. Clean. Prod.* **2025**, *494*, 144939. [CrossRef]
23. He, P.; Jin, J.G.; Pan, W.; Chen, J. Route, speed, and bunkering optimization for LNG-fueled tramp ship with alternative bunkering ports. *Ocean Eng.* **2024**, *305*, 117957. [CrossRef]
24. Shih, Y.C.; Tzeng, Y.A.; Cheng, C.W.; Huang, C.H. Speed and fuel ratio optimization for a dual-fuel ship to minimize its carbon emissions and cost. *J. Mar. Sci. Eng.* **2023**, *11*, 758. [CrossRef]
25. Livaniou, S.; Papadopoulos, G.A. Liquefied natural gas (LNG) as a transitional choice replacing marine conventional fuels (heavy fuel oil/marine diesel oil), towards the era of decarbonization. *Sustainability* **2022**, *14*, 16364. [CrossRef]
26. Kuittinen, N.; Heikkilä, M.; Jalkanen, J.P.; Aakko-Saksa, P.; Lehtoranta, K. Methane slip emissions from LNG vessels. In Proceedings of the 30th CIMAC Congress, Busan, Republic of Korea, 12–16 June 2023; p. 629.
27. Lim, T.W.; Hwang, D.H.; Choi, Y.S. Design and optimization of a steam methane reformer for ship-based hydrogen production on LNG-fueled ship. *Appl. Therm. Eng.* **2024**, *243*, 122588. [CrossRef]
28. Kuittinen, N.; Koponen, P.; Vesala, H.; Lehtoranta, K. Methane slip and other emissions from newbuild LNG engine under real-world operation of a state-of-the art cruise ship. *Atmos. Environ. X* **2024**, *23*, 100285. [CrossRef]
29. Zarrinkolah, M.T.; Hosseini, V. Methane slip reduction of conventional dual-fuel natural gas diesel engine using direct fuel injection management and alternative combustion modes. *Fuel* **2023**, *331*, 125775. [CrossRef]
30. Shangguan, Y.; Tian, X.; Pang, K.W.; Wang, S. Optimizing dual-fuel ship operations considering methane slip. *Transp. Res. Part B Methodol.* **2025**, *198*, 103247. [CrossRef]
31. Wu, Y.; Huang, Y.; Wang, H.; Zhen, L. Joint planning of fleet deployment, ship refueling, and speed optimization for dual-fuel ships considering methane slip. *J. Mar. Sci. Eng.* **2022**, *10*, 1690. [CrossRef]

32. Maloberti, L.; Zaccone, R.; De Gaetano, J.; Campora, U. A comparison among innovative hybrid propulsion systems to reduce the environmental impact of a small passenger ship. *Sustain. Energy Technol. Assess.* **2025**, *75*, 104194. [CrossRef]
33. Milićević, S.; Blagojević, I.; Milojević, S.; Bukvić, M.; Stojanović, B. Numerical analysis of optimal hybridization in parallel hybrid electric powertrains for tracked vehicles. *Energies* **2024**, *17*, 3531. [CrossRef]
34. Sun, M.; Vortia, M.P.; Xiao, G.; Yang, J. Carbon policies and liner speed optimization: Comparisons of carbon trading and carbon tax combined with the European union emissions trading scheme. *J. Mar. Sci. Eng.* **2025**, *13*, 204. [CrossRef]
35. Tan, R.; Psaraftis, H.N.; Wang, D.Z. The speed limit debate: Optimal speed concepts revisited under a multi-fuel regime. *Transp. Res. D Transp. Environ.* **2022**, *111*, 103445. [CrossRef]
36. Ma, D.; Ma, W.; Jin, S.; Ma, X. Method for simultaneously optimizing ship route and speed with emission control areas. *Ocean Eng.* **2020**, *202*, 107170. [CrossRef]
37. Wang, C.; Liu, X.; Zhou, Y.; Qian, J. Optimization of speed and refueling strategy for liner shipping companies considering refueling at OPL. *Reg. Stud. Mar. Sci.* **2025**, *89*, 104355. [CrossRef]
38. Zhao, Q.; De, A.; Allmendinger, R. Optimization of a dual-fuel engine bunker fuel management strategy. *IFAC-Pap.* **2025**, *59*, 1113–1118. [CrossRef]
39. Sheng, D.; Jiang, J.; Wang, H.; Tan, Z.; Wang, Y. Optimal compliance choices for ocean carriers under the sulphur regulation. *Transp. Res. Part D Transp. Environ.* **2023**, *116*, 103639. [CrossRef]
40. Fan, L.; Gu, B.; Luo, M. A cost-benefit analysis of fuel-switching vs. hybrid scrubber installation: A Contain. Route Through Chin. SECA case. *Transp. Policy* **2020**, *99*, 336–344. [CrossRef]
41. Sun, L.; Wang, X.; Hu, Z.; Ning, Z. Carbon and cost accounting for liner shipping under the European Union Emission Trading System. *Front. Mar. Sci.* **2024**, *11*, 1291968. [CrossRef]
42. Spoof-Tuomi, K.; Niemi, S. Environmental and economic evaluation of fuel choices for short sea shipping. *Clean Technol.* **2020**, *2*, 34–52. [CrossRef]
43. Tan, R.; Duru, O.; Thepsithar, P. Assessment of relative fuel cost for dual fuel marine engines along major Asian container shipping routes. *Transp. Res. Part E Logist. Transp. Rev.* **2020**, *140*, 102004. [CrossRef]
44. Merien-Paul, R.H.; Enshaei, H.; Jayasinghe, S.G. Effects of fuel-specific energy and operational demands on cost/emission estimates: A case study on heavy fuel-oil vs liquefied natural gas. *Transp. Res. Part D Transp. Environ.* **2019**, *69*, 77–89. [CrossRef]
45. Lan, X.; Zuo, X.; Tao, Q. Container shipping optimization under different carbon emission policies: A case study. *Sustainability* **2023**, *15*, 8388. [CrossRef]
46. Zhao, S.; Duan, J.; Li, D.; Yang, H. Vessel scheduling and bunker management with speed deviations for liner shipping in the presence of collaborative agreements. *IEEE Access.* **2022**, *10*, 107669–107684. [CrossRef]
47. Dulebenets, M.A. Green vessel scheduling in liner shipping: Modeling carbon dioxide emission costs in sea and at ports of call. *Int. J. Transp. Sci. Technol.* **2018**, *7*, 26–44. [CrossRef]
48. Yao, Z.; Ng, S.H.; Lee, L.H. A study on bunker fuel management for the shipping liner services. *Comput. Oper. Res.* **2012**, *39*, 1160–1172. [CrossRef]